14

Dynamic Mass Measurement Techniques

Kenneth Williams

U.S. Bureau of Mines
Pittsburgh, PA, U.S.A.

Chuck Fairchild

Health, Safety, and Environment Division
Los Alamos National Laboratory
Los Alamos, NM, U.S.A.

and

Joseph Jaklevic

Lawrence Berkeley Laboratory
University of California,
Berkeley, CA, U.S.A.

INTRODUCTION

This chapter describes three techniques for aerosol mass measurement, each of which could be most appropriately described as a short-term batch process. Only one of them approaches the instantaneous measurements characteristic of optical or light-scattering techniques, but all of them can determine the mass of collected aerosol samples in intervals convenient for many applications. These three techniques are the beta gauge, piezoelectric crystal, and tapered-element oscillating microbalance (TEOM®). These techniques have been used to measure a variety of aerosols. Various applications of the measurement techniques are discussed or referenced in the text.

BETA GAUGE METHOD

Measurement Principles

The beta gauge method of mass determination depends upon the near exponential decrease in the number of beta particles transmitted through a thin sample as the areal density is increased. The beta particles are emitted as a continuum energy distribution by a radioisotope source and their intensity is measured with a suitable electron counter. The method has the advantages of instrumental simplicity and ease of automation for large-scale applications. The dynamic range of sensitivity is well matched to the mass range normally of interest in aerosol monitoring in which thin membrane filters are the

However, a detailed understand- parameters which affect the meas- is necessary in order to ensure instrumental implementation and interpretation of results.

14-1 is a schematic diagram of a beta gauge instrument consisting of the source, detector, and sample. A consists of determining the in a continuous beta particle spec- by the radioisotopic source and through the sample. Under the experimental conditions, the trans- flux (I) is related to the sample mass the relationship (Evans 1955)

$$I = I_0 e^{-\mu x} \tag{14-1}$$

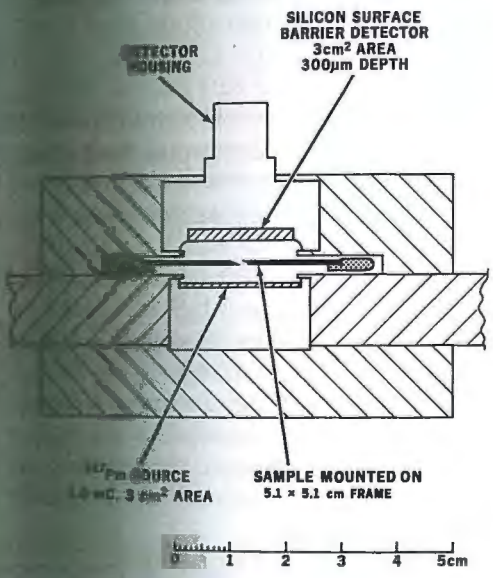

Schematic Diagram of a Beta-Gauge Measuring Thin Aerosol Samples.

where I_0 is the incident flux, μ is the mass absorption coefficient for beta absorption (cm^2/g), and x is the mass thickness of the sample (g/cm^2). The mass absorption coefficient is normally determined through a calibration procedure involving the measurement of a series of known standards which bracket the mass range of interest (Jaklevic et al. 1981). The incident flux, I_0, can either be derived during the same calibration procedure or, if the interval between successive measurements is short, the value of I_0 can be made to cancel by calculating the ratio between transmitted fluxes measured with and without the particle deposit. The latter case applies for certain beta gauge designs where continuous particle deposition is monitored (Macias and Husar 1970).

Instrument Design

The optimal choice of source and detector depends upon many factors. The radioisotope source must have beta particle emission as the dominant mode of decay and exhibit half-life sufficient for the large decay corrections or frequent source replacements to be unnecessary. The source strength should provide adequate precision in counting statistics within the limitations of the detector rate-handling capabilities. Finally, as discussed in more detail below, the energy of the beta spectrum must be chosen to produce a mass absorption coefficient matched to the range of thicknesses to be measured. Table 14-1 lists a selection of radioisotopes appropriate for aerosol beta gauge applications together with relevant parameters for each (Lilienfeld 1975).

Commonly Available Sources Suitable for Beta Attenuation Measurements

Half-Life (years)	E_{max} (MeV)	Range (mg/cm^2) in Carbon at E_{max}	Range (mg/cm^2) in Carbon at $E_{aver} = 0.4E_{max}$
92	0.067	7.7	1.6
5730	0.156	32	6.6
2.62	0.225	60	13
10.76	0.67	290	77
3.1×10^4	0.712	320	84
3.8	0.765	340	94

The detector must be sensitive to the beta particles (i.e., electrons) in the energy range of interest and capable of operation at a counting rate sufficient to perform measurements in the required time interval. Beta gauges have been operated using a variety of detector types, including ionization chambers (Husar 1974), Geiger–Muller tubes (Gleason, Taylor, and Tabern 1951; Lilienfeld 1975; Klein, Ranty, and Sowa 1984), scintillation spectrometers (Jaklevic, Madden, and Wiegand 1983), and semiconductor diode detectors (Macias and Husar 1970; Jaklevic et al. 1981). Of equal importance is the choice of associated pulse processing electronics. Depending upon the type of detector used, it may be necessary to employ a preamplifier, amplifier, and pulse amplitude discriminator. Because of the level of precision required in many measurements, these analogue signal processing components must be selected and tested for long-term stability and reliability. For those laboratory applications where extreme limits of precision and accuracy are the objective, temperature stabilization of the operating environment is recommended. Most recent beta gauge systems employ semiconductor diode detectors and solid state pulse processing electronics because of their simplicity and stability of operation. The following discussion will be oriented toward this type of system although most of the comments also apply to other types of detectors.

The source–detector geometry must be maintained in a stable mechanical configuration to minimize spurious counting-rate variations. Also, it is important that the spacing be as close as possible in order that changes in atmospheric density within the gap are not interpreted as mass variations in the sample (Courtney, Shaw, and Dzubay 1982). The lower limit to the spacing is normally determined by the thickness of sample holders and the associated handling mechanisms used with automated instrumentation.

Theoretical Considerations

Studies have shown that the functional dependence of beta particle transmission expressed in Eq. 14-1 is not valid for precise experimental measurements (Jaklevic et al. 1981; Macias and Husar 1970; Heintzenberg and Winkler 1984). This result is not unexpected since the exponential behavior is not a reflection of fundamental mechanisms associated with beta particle attenuation in matter. Electrons with kinetic energies less than 1 MeV lose energy primarily through elastic collisions with atomic electrons present in the sample. As a consequence, an electron with a well-defined initial energy distribution will slow down through a series of discrete energy losses as it traverses the sample. An incident electron beam with a well-defined initial energy and direction will experience a gradual decrease in the average energy, accompanied by a spreading in the distribution of the beta ray's energy and angle of incidence on the target material.

The radioisotopic beta particle emission process results in a continuum of electron energies. Figure 14-2 is an idealized representation of a measured beta spectrum from a typical source. The energy distribution extends from a minimum energy determined by the source window thickness to a maximum endpoint energy, E_{max}, which is the total energy available for the radioactive decay process. An electronic discriminator level, E_{disc}, has been indicated above a low-energy electronic noise tail. As the mass between source and detector is increased, the counting rate observed above this discriminator level in the

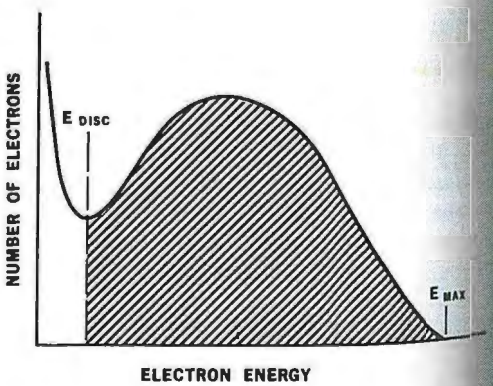

FIGURE 14-2. Idealized Beta Particle Spectrum Emitted from a Radioisotope Source.

detector represents those electrons ... original continuum spectrum that have ... totally stopped in the sample and ... incident on the detector. This rate ... complex energy loss process which ... on several variables, including the ... energy of the electrons in the beta ... and the amount of material traver- ... When averaged over all these effects, the ... dependence of the counting rate on ... thickness traversed is approximately ex- ... Repeated measurements in a care- ... defined experimental geometry using ... absorbers have established an ... relationship between the mass ... coefficient in Eq. 14-1 and the ... spectrum endpoint energy (Gleason, ... and Tabern 1951):

$$\mu\,(\mathrm{cm}^2/\mathrm{g}) = 0.017 E_{\max}^{-1.43} \qquad (14\text{-}2)$$

... there is a considerable variation ... various investigators regarding the ... coefficients reflecting the empir- ... nature of these parameters (Sem and ... 1975).

... beta particle energy-loss process ... scattering from atomic electrons ... than nuclei, there is the possibility of ... additional dependence of the absorption ... on the average atomic number of ... samples. Various authors have studied ... effect and an empirical relationship has ... derived (Klein, Ranty, and Sowa 1984):

$$\mu\,(\mathrm{cm}^2/\mathrm{g}) = 0.016(Z/A)^{4/3} E_{\max}^{-1.37} \qquad (14\text{-}3)$$

... Z is the atomic number and A is the ... weight. However, the validity of this ... relationship seems to depend on the specific ... of the beta gauge. A less dramatic ... dependence of attenuation on Z/A has been ... observed by Jaklevic et al. (1981) and at- ... to the relative importance of the ... angular distribution in the particular ... source-detector arrangement employed in ... study. Regardless of the details of func- ... dependence, it should be noted that ... associated with this effect are ... considerable since the range of Z/A is small for all elements, with the exception of hydrogen.

The practical consequences of these theoretical observations are that, although estimates of beta gauge sensitivity can be obtained using generalized expressions, precise mass measurements require that each specific instrument is calibrated using known gravimetric standards. It is also necessary to limit the dynamic range over which one attempts to apply a given calibration using a strictly exponential approximation. To the extent that the deposited mass is normally a small fraction of the tare weight of the filter medium, this is not a severe limitation in aerosol applications.

A more complete understanding of precision and accuracy requires a detailed error analysis. If one assumes that the value of μ has been carefully determined and that the counting interval is known with complete certainty, then the precision of the mass measurement is determined by experimental variations in the determination of I_0 and I. Using Eq. 14-1, the root mean square error, $\sigma^2(x)$, in the calculated concentration, x, can be derived as (Cooper 1975)

$$\sigma^2(x) = \frac{1}{\mu^2}\left[\frac{\sigma^2(I_0)}{I_0^2} + \frac{\sigma^2(I)}{I^2}\right] \qquad (14\text{-}4)$$

where I_0 and I are the incident and transmitted fluxes integrated for a fixed time interval. For the case where the errors associated with I and I_0 are the result of Poisson counting statistics only, i.e., $\sigma(I) = (I)^{1/2}$, and if the counting intervals of the two measurements are equal, the precision $\sigma(x)$ for a difference measurement varies as the inverse of the mass absorption coefficient and the inverse square root of measurement interval, as might be expected. The inverse dependence of precision on mass absorption coefficient supports the intuitive observation that lower-energy beta spectra will provide a more sensitive indicator of small mass changes in the sample. On the other hand, if the energy is too low, the exponential approximation is no longer valid since an increasing fraction of beta particles is totally stopped in the sample. Referring to

Table 14-1, a useful rule of thumb is to select a beta spectral average energy corresponding to a range which is several times the maximum thickness to be measured. For this reason, most beta gauges designed for aerosol monitoring employ either ^{14}C or ^{147}Pm as reasonable choices for use with substrates in the range 10–100 mg/cm^2 and deposits in the range 20–500 μg/cm^2 (Klein, Ranty, and Sowa 1984).

The derivation of Eq. 14-4 assumed that the value of the mass absorption coefficient was known from a previous calibration procedure. However, the value of the mass absorption coefficient is normally calculated from transmission measurements performed on a series of mass standards which bracket the anticipated range of operation of the instrument. A more complete error analysis including uncertainties in the fitting procedure is discussed by Jaklevic et al. (1981). A general conclusion of this analysis is that, although the absolute accuracy of a mass measurement is affected by such calibration errors, the precision is dominated by the variability in the determinations of I and I_0. In principle, the precision of a given mass determination can be improved by increasing the counting interval to reduce the relative error associated with Poisson counting statistics. However, one eventually reaches a limit where the variability in the measured counting rate is dominated by other effects which are not easily controlled. Sources of systematic errors can include fluctuations in atmospheric density, changes in laboratory relative humidity, which can affect the substrate mass for hygroscopic media, instabilities in the mechanical design and variability in the placement of the sample in the instrument (Courtney, Shaw, and Dzubay 1982). A major source of instrumental instability is the result of long- and short-term drift in the detector and analogue pulse processing electronics. Although modern solid state circuits can have temperature coefficients approaching 1 part in 10^4 per degree Celsius, the demands placed on precision beta gauge measurements can approach this level even in temperature-controlled environments. Because of the difficulty in controlling such sources of errors, it should be a requirement in all beta gauge measurement protocols that recalibration of the instrument be performed before each series of measurements and that replicate samples be repeatedly analyzed at the same time as the unknowns in order to monitor instrumental stability.

Potential Biases

The near exponential behavior of the beta absorption process and the variations discussed above can result in several potential measurement artifacts which should be understood. Principal among these are particle size effects, substrate inhomogeneities and atomic number dependence.

Particle size effects result from the fact that the beta gauge transmission measurement represent an average of the absorption experienced by an aggregate of particles deposited on the filter substrate. In the limit where this deposition is a homogeneous layer of small particles whose average diameter is much less than the layer thickness, the interpretation of the results in terms of exponential absorption by a uniform deposit is valid. On the other hand, one can imagine a deposit of equivalent mass but consisting of only a few, very massive particles. In an extreme manifestation of this latter case, there could exist total absorption within a given particle. The transmission measurement in this limiting case would then reflect the fractional area covered by the particles, and interpretation in terms of an exponential absorption by a uniform deposit would be invalid.

A detailed discussion of this problem for the general case of exponential absorption is given by Cooper (1976). A similar treatment using a simplified model applied to the case of aerosol particles is given by Jaklevic et al. (1981). Figure 14-3 is a plot of the discrepancy attributed to this phenomenon for the case of a 100 μg/cm^2 deposit of unit-density particles. The ratio of the mass as determined from beta gauge measurement to the true gravimetric mass is plotted as a function of the linear

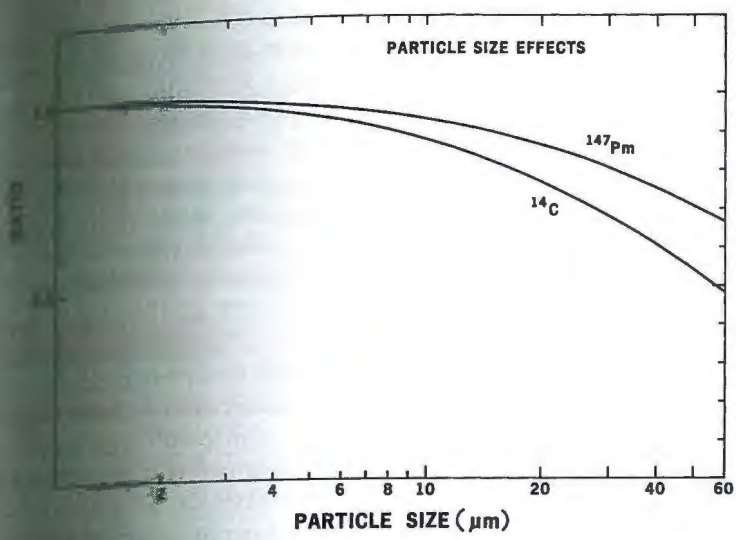

FIGURE 14-3. The Discrepancy in Beta Gauge Mass Measurements as a Function of Particle Size for the Case of Two Commonly Used Isotopes.

particles. The discrepancy between the two increases for large particles at a rate which is greater for the source with the larger absorption coefficient.

These results indicate that one must either limit the size distribution to particles below 10 μm diameter or, if larger particles are to be analyzed, ensure that the average deposit thickness is sufficient for a statistically meaningful number of particles to be present. Similarly, for impaction samples, the deposit thickness must be uniform over the measurement area to a degree where the average of the exponential is equal to the exponential of the average.

An effect which can be explained using similar logic has to do with discrepancies caused by filter and source inhomogeneities. A microscopic examination of most membrane filter media shows that the substrate consists of a nonuniform distribution of fibers or flocculated material with relatively open spaces in between. Similarly, a radioisotope source is normally fabricated by methods which result in local inhomogeneities in the radioactivity across the face of the source. Although a point source can, in principle, alleviate this problem, there is a practical limit to the specific activity that can be concentrated in a small volume. Variations in the apparent mass of the substrate can result from random alignments between the respective inhomogeneities causing spurious high or low mass readings. The problem is exacerbated by the large mass of the substrate relative to the deposit. Since neither the source nor the substrate can be made to be perfectly spatially uniform, it is important to constrain the measurement protocol to position the filter in the instrument identically for both the initial and final weighings. This is most easily implemented in the case of large-scale automated systems and is necessary for mass measurements which aspire to achieve the limits of instrumental precision (Courtney, Shaw, and Dzubay 1982).

The atomic number dependence of the mass absorption coefficient requires that certain precautions be taken regarding the choice of calibration standards and in the interpretation of results from discrete pollution sources. Table 14-2 shows the Z/A values for a list of compounds commonly observed in ambient aerosol sampling. The mass absorption coefficients are calculated using both the Z/A dependence observed by Jaklevic et al. (1981) and those calculated from Eq. 14-3. The mass absorption coefficient for

TABLE 14-2 Effect of Atomic Number Dependence on the Measured Mass of Several Compounds

Compound	Z/A	μ (cm^2/mg)[a]	μ (cm^2/mg)[b]
$(NH_4)_2SO_4$	0.530	0.153	0.166
$NH_4H\ SO_4$	0.521	0.152	0.163
$CaSO_4 \cdot H_2O$	0.511	0.152	0.159
SiO_2	0.499	0.154	0.154
$CaCO_3$	0.500	0.154	0.154
Carbon	0.500	0.154	0.154
Fe_2O_3	0.476	0.163	0.144
NaCl	0.478	0.172	0.145
$PbSO_4$	0.429	0.193	0.126
$PbCl_2$	0.417	0.204	0.121
PbBrCl	0.415	0.206	0.120

a. From Jaklevic et al. (1981)
b. Z/A dependence calculated from Eq. 14-3. Values normalized to 0.154 for carbon to account for instrumental differences

a mixture of compounds would be the weighted sum of the respective coefficients. It is obvious that an inappropriate choice of calibration foils can affect the accuracy of the measurements if not corrected for in the data analysis. Similarly, measurements of a set of samples in which the relative contribution of diverging Z/A compounds varies widely will need special consideration in the interpretation. Although a complete correction requires that the sample composition be known, some estimate of the probable error can be obtained by observing the range of values of μ for the compounds listed in Table 14-2 and incorporating an error analysis based on Eq. 14-1. It should be noted that the errors associated with Z/A variations affect the accuracy of the measurements but not the precision and, as a consequence, have little effect on the lower limit of sensitivity of the beta gauge method.

Results and Applications

In the literature there exist descriptions of a number of beta gauge designs optimized for specific particle monitoring applications. In general, a distinction can be made between those made for continuous monitoring of discrete sources or ambient aerosols and those designed for precision laboratory analysis of collected particles. In on-line monitoring applications, it is difficult to control the systematic errors associated with a variability in the tare weight and nonuniformities in the substrate mass. Such systems usually exhibit a root mean square precision of the order of 25 μg/cm^2 (Macias and Husar 1970; Husar 1974). In laboratory-based systems where calibrations are frequently performed, tare weights are individually measured and systematic effects such as sample placement are reduced; it is possible to achieve precisions of 3 μg/cm^2 for individual mass measurements, corresponding to a precision of difference measurements of 5 μg/cm^2 (Courtney, Shaw, and Dzubay 1982; Jaklevic et al. 1981). However, there are a number of criteria other than precision and individual designs which need to be evaluated in terms of specific applications. These incude speed, convenience, cost, operating environment, and automation operation.

Beta gauge mass measurements have been incorporated into a number of studies. Loo et al. (1978) report the use of a beta gauge to

TABLE 14-3 List of Commercial Sources

Code	Address
MST	MST Measurement Systems, Inc. 327 Messner Dr., Wheeling, IL 60090 U.S.A. (Beta attenuation devices)
WAI	Wedding and Associates, Inc., P.O. Box 1756, Fort Collins, CO 80522, U.S.A. (Beta attenuation devices)
AII	Andersen Instruments Inc., 4801 Fulton Industrial Blvd., Atlanta, GA 30336, U.S.A. (Beta attenuation devices)
BCI	Berkeley Controls, Inc., 2825 Laguna Canyon Rd., Laguna Beach, CA 92652, U.S.A. (QCM cascade impactor)
CMI	California Measurements, Inc., 150 E. Montecito Ave., Sierra Madre, CA 91024, U.S.A. (QCM cascade impactor)
FTM	Femtometrics, 1721 Whittier Ave, Suite A, Costa Mesa, CA 92627, U.S.A. (SAW microbalance)
TSI	TSI, Inc., P.O. Box 64394, 500 Cardigan Road, St. Paul, MN 55164, U.S.A. (QCM aerosol mass monitor)

the mass of aerosols collected on oster filters as part of a large-scale program in St. Louis. They report a of 5 μg/cm² for substrate masses of of 20 mg/cm². Stevens et al. (1980) beta gauge mass determinations for collected on polytetrafluoroethylene th average areal densities of less /cm². Spengler and Thurston cribe the use of beta gauge measure- in an extensive indoor air pollution Recent applications using continuous monitors have been described by Klein, and Sowa (1984), and Heintzenberg (1984). Table 14-3 lists the com- urces of several beta attenuation nts.

ECTRIC CRYSTAL MENT METHOD

ment Principles

crystalline materials, when mechan- ssed in compression or tension, re- by producing an electromotive force or proportional to the stress along speci- crystal planes. This phenomenon is the oelectric strain gages. Likewise, material when subjected to an field across certain crystal planes by mechanically expanding or contracting. Thus, a rapidly alternating field or voltage produces physical oscillation or in a piezoelectric crystal. The vibra- ncy depends on the orientation ic field with respect to the major rystal and, for certain modes of on the thickness and density of the ost important for their application ctric microbalances, the natural frequency also depends on the mass stal.

ease of mass on sensitive planes, or of a piezoelectric crystal causes the onant frequency to decrease in tion to the increased mass. The bility at a constant mass and the to the mass of the vibrating crystal its aerosol measurement capability. The sensitivity is proportional to the square of the vibrational frequency, f_0, of the crystal in its fundamental mode:

$$\Delta f = K_\alpha f_0^2 \frac{\Delta m}{A} \tag{14-5}$$

where K_α is a constant and $\Delta m/A$ is the area sensitivity as mass change per unit area producing a frequency change Δf. Sensitivities of $\sim 10^9$ Hz/g for optimized crystal geometries are typical, and a stability of ± 0.5 Hz at 10 MHz is attainable. Advantage has been taken of these properties of peizoelectric crystals to create a class of instruments sensitive to mass, or changes in mass, that are generally called quartz crystal microbalances (QCM). The piezoelectric sensor principle and its application to the QCM, as well as other types of instruments, are discussed in some depth by Ward and Buttry (1990). A review of the limitations of piezoelectric crystals in aerosol measurement is provided by Lundgren, Carter, and Daley (1976).

Piezoelectric quartz crystals used in most aerosol sampling QCMs are cut and polished on specific crystallographic planes called the AT planes. AT-cut crystals oscillate in a thickness-shear mode, that is, the oscillation occurs between two AT-cut surfaces, through the body of the crystal. In this mode, a single vibrational node is at the midplane between the two major surfaces of the thin, disk-shaped crystal. The driving electrodes are circular metallic coatings electroplated on each opposite major surface of the crystal. Oscillation occurs only in that portion of the crystal lying in the electric field between the electrode boundaries. The sensors then vibrate at a frequency proportional to the mass of the crystal and electrodes plus the mass of particles that adhere to the collecting metallic electrode surface. Particles attached to the surface of the crystal outside the electrode area have little effect on the vibrating portion of the crystal and are not detected.

Sampling Methods

A simple QCM aerosol sampler designed to measure total or respirable particle mass is

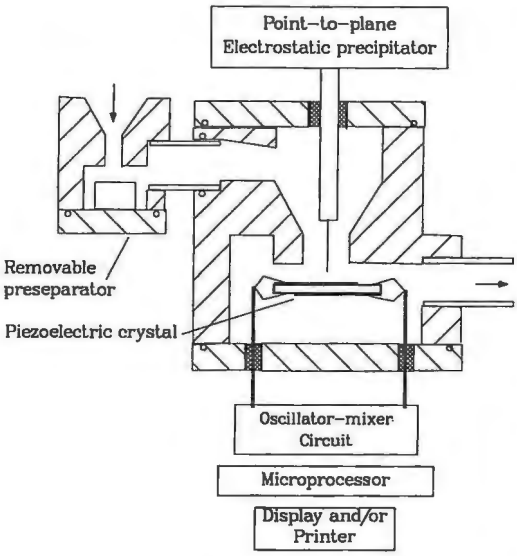

FIGURE 14-4. A Typical Sampling Arrangement for a QCM Aerosol Sampler. The Oscillator–Mixer Circuit Contains a Reference Crystal Identical to the Collection Crystal.

illustrated schematically in Fig. 14-4. The preselector at the inlet collects large particles by impaction. Respirable aerosol passes to the collection crystal, where the particles get deposited by electrostatic precipitation. The crystal (typically a 1 cm diameter by 1 mm thick disk) is suspended by posts and frames that also act as electrical conductors. Denuded air is exhausted by a pump. Both the impactor and the collection crystal are removable for cleaning, or a provision may be made for cleaning in situ.

QCM aerosol samplers may collect particles by electrostatic precipitation, inertial impaction, or other methods. In all methods, the particles are deposited onto the metal-coated quartz crystal surface. The clean crystal substrate vibrates at a natural harmonic frequency usually between 5 and 10 MHz. As material is deposited on its surface, the frequency of vibration of the crystal decreases in proportion to the mass of the deposit. A separate, matched crystal, which is protected from particle deposition but is in the same thermal and flow environment, is installed to provide a stable reference vibrational frequency. There is some evidence, however, that the reference crystal often is not in thermal equilibrium with the collection crystal (Sem and Tsurubayashi 1975). Signals produced by the two crystals are electronically mixed to provide a difference, or beat, frequency between the two. This beat frequency is an indicator of the mass of material collected. In most commercially available samplers either the beat frequency or the calculated mass can be displayed.

Potential Biases

Calibration

Initial calibration of a QCM aerosol sampler is normally performed by the manufacturer who sets the display to correspond to a measured aerosol concentration for known changes in the frequency of vibration of the quartz crystal. After factory calibration sample mass concentration can be calculated from the measured beat frequency, aerosol volume flow rate, mass sensitivity determined from the calibration, and sampling time. However, the instrument should be calibrated by the user against a well-characterized aerosol such as polystyrene latex (PSL) spheres or, if possible, against the expected challenge aerosols. Measurements can vary for different aerosols for several reasons.

Particle Size Effects

Both the mass collection and measurement efficiency may be affected by particle size. Collection efficiency is a function of the collection method, particle size distribution, and the substrate, or crystal surface. Collection methods such as impaction or electrostatic precipitation are discussed thoroughly elsewhere, but the collection efficiency of the crystal surfaces is of interest here. On a macroscale, the metallic electrode collecting surface is a smooth, hard surface, as are many bare impaction or other collection surfaces. Large, elastic particles may bounce, or may be reentrained from such surfaces after deposition. This is especially true in QCM impactors, where collection is due to inertial forces. An examination of the surfaces from a multistage impactor collection crystal has shown

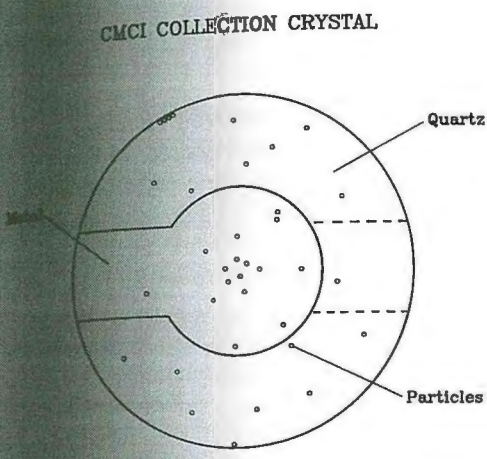

FIGURE 14-5. Typical Large, Spherical Particle Collection Pattern for Stages 1 and 2. Crystal Diameter is ~ 1 cm. (By Permission, Fairchild and Wheat 1984.)

that large, spherical particles may also migrate across the surface (Fig. 14-5, Fairchild and Wheat 1984). Bounce or migration may be eliminated or decreased by applying a soft or sticky coating to the surface. Because of the sensitivity of the piezoelectric impactor stage, the coating must be strictly controlled by following the manufacturer's instructions.

Adherence Effects

The detection of particles collected on even a coated surface may suffer another problem not observed in other samplers. Detection of the increased mass depends upon good coupling, or attachment, to the surface. Coupling is a function of the adherence of particles to the surface and can be a problem regardless of the collection technique. Simply put, the deposit mass must vibrate in unison with the collection crystal in order to be measured properly. Poor coupling generally occurs with thicker deposits. Often, its occurrence may be detected if the change in frequency is plotted as a function of time, while maintaining a uniform deposition rate. The frequency change becomes nonlinear with increase in deposit mass as the coupling decreases. Also, loss of sensitivity tends to increase with particle size above a few micrometers.

A related problem results from a variation in sensitivity of the electrode across its surface. As stated earlier, the deposit must rest on the metal electrode to be correctly sensed. Actually, the electrode itself may not be uniformly sensitive over its area because of crystal defects or electric field aberrations. This variation is corrected empirically in initial calibration but may be a source of small error if periodic recalibration is not done.

Overloading

For a relatively large collected mass, even if well attached, "saturation" of the crystal may cause severe nonlinearity. Excessive collected mass may cause a condition of gross overloading in which the vibration of the sensing crystal ceases altogether. The procedures to prevent overloading, such as periodic cleaning, are normally discussed in the instruction manuals.

Particle Losses

The QCM aerosol samplers are subject to particle losses to inlet and internal surfaces just as other aerosol samplers. Careful design can reduce these losses, but some loss is likely. Therefore, the losses should be characterized before use. Although little detailed data are available, the QCM cascade impactors presently available are particularly susceptible to wall losses. They collect a wide range of particle sizes, have a comparatively large ratio of interstage volume to flow rate (long airborne particle residence time), and have internal surface irregularities that present an opportunity for turbulence generation and particle deposition—all features conducive to wall loss.

Results and Applications

Industrial Hygiene Aerosol Sampling

At least one QCM instrument, called an aerosol mass monitor (Model 8510, TSI Inc., St. Paul, MN), is available to measure aerosols in inhalation hazard assessment. Either total dust or respirable dust concentrations common to many workplaces can be determined

in a 24 s or 2 min sampling period, depending upon the expected concentration. For the measurement of respirable aerosols a single-stage impactor with a 50% effective cutoff aerodynamic diameter (d_{50}) of 3.5 μm is installed in the sampling airstream ahead of the collection crystal. Because the collection efficiency of this impactor does not match the characteristics of the ACGIH respirable dust curve (Lippmann 1978) closely, the mass monitor estimates the respirable mass concentration best for aerosols that are > 50% respirable.

In this instrument, particles are deposited on the crystal by electrostatic precipitation. A mechanism is incorporated to clean the collection crystal between samples without removing or disturbing the crystal. After the cleaning procedure, the beat frequency may be displayed to ensure that the crystal is clean and approximates its original vibrational frequency. The data reduction and the display modules are packaged together with the collection system and battery in a portable unit weighing 5 kg.

Fairchild, Tillery, and Ettinger (1980) evaluated the performance of an early version of this mass monitor against several aerosols. They reported that the mass monitor did not measure the air concentration of different aerosols equally well, and that the instrument measured the concentration of solid particles greater than 6 μm diameter poorly. It did provide a reliable measurement of small solid particle and liquid particle aerosols, particularly when multiple samples were averaged. For most industrial aerosols, the mass monitor measured the respirable concentration more accurately than the total aerosol concentration, presumably because of the better adherence and retention of the smaller particles by the sensing crystal.

The piezoelectric mass monitor, because of its mass sensitivity and short response time, allows a quick measurement of aerosol concentration, within the limitations described. It should be used primarily with respirable-size particles because it reportedly measures large particles poorly. The potential errors suggest that it be used as a survey instrument, or in cases where a number of samples can be averaged.

Near-Real-Time Cascade Impactors

Cascade impactors that operate with multiple sets of paired piezoelectric crystals—one set for each impaction stage—are available. These can be used in some environmental, industrial hygiene, clean room, and other field sampling applications, but are usually used in research applications. These impactors are inconvenient and somewhat complex for routine purposes, but they do provide a rapid indication of size distribution as well as mass concentration.

QCM impactors with ten stages have been available for a number of years (Model C-1000A, QCM Research, Laguna Beach, CA; PC-2, California Measurements, Inc., Sierra Madre, CA) and cascade impactors with fewer stages are now appearing on the market (Models MPS-3, MPS-4GL, California Measurements, Inc., Sierra Madre, CA). Figure 14-6 shows one ten-stage cascade impactor along with its separate data reduction and display module. The two modules are connected by cabling to transmit power and signals and, in some cases, to control the main valve admitting aerosol into the stages. When the valve is closed, only filtered air flows through the stages. An aerosol sample is admitted by opening the valve, usually for a measured length of time. After the valve is closed, clean air again flows into the instrument. Approximately 30 s are required for the sample to pass through all stages because of the low flow rate and large interstage volume. After a short delay, the operator may print the frequency change for each stage, the computed mass collected by each stage, and a histogram of the size distribution.

Calibration of the individual stages of this cascade impactor was performed with unit- and known density aerosols (Fairchild and Wheat 1984). They reported the stage d_{50} values to be somewhat different from the manufacturer's values. They also reported significant particle losses in the impactor, both for particles smaller than $d_a = 0.4$ μm and for particles larger than $d_a = 3$ μm.

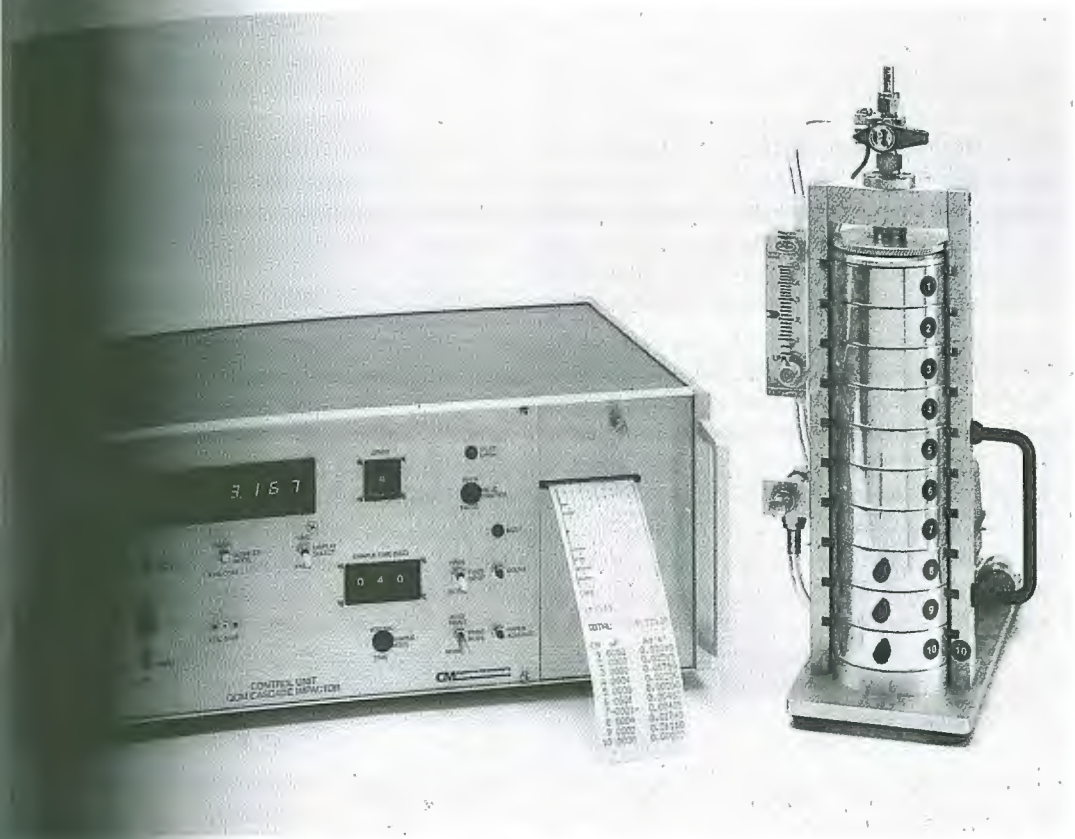

14-6. A QCM Cascade Impactor Showing the Impactor Stack on The Data Acquisition, Display, and Print Unit on the Left. (By Permission CMI, Table 14-3.)

Cascade impaction devices have been ospheric and environmental sam- applications (Rose et al. 1979; Wallace Chuan 1977). For these applications the have been mounted inside aircraft and namically shaped containers at- to aircraft wings. Karasek (1978) out that piezoelectric crystal sub- are also suitable substrates in many the examination of collected aero- light and electron microscopy.

coustic Wave Microbalances

recently developed QCM aerosol nt has a mass sensitivity much than samplers with AT-cut crystals. rease in sensitivity results from modifi- to the quartz crystal and its mode of n. Instead of producing an electric field through the crystal thickness, the electric field is applied between electrodes on the same surface. Provided a separation of no more than several micrometers between electrodes can be achieved, this mode of excitation results in a vibrational frequency of up to 300 MHz. Theoretically, a mass sensitivity may be obtained that is three orders of magnitude greater than in the AT-cut crystal devices (Bowers and Chuan 1989). The vibrational mode along one surface is called the surface acoustic wave (SAW) mode.

Commonly, several driver electrodes are deposited in an interdigital pattern on the crystal at separations of $\sim 15\ \mu m$ between positive and negative branches. This distance produces standing-wave vibrational frequencies of about 100 MHz. Because its sensitivity is proportional to the vibrational frequency

squared (Eq. 14-5), the increased sensitivity of a SAW device operating at 100 MHz over a device operating at 10 MHz is theoretically a factor of 100. Mass sensitivities in the range 10^{10}–10^{11} Hz/g appear to be attainable with the SAW devices.

As in other QCM aerosol samplers, an overloading of the active crystal is one limiting consideration for the SAW microbalances; at their oscillation frequency, saturation damping occurs at very small mass. Short aerosol collection time, very dilute air concentrations, and thin surface deposits are necessary to prevent damping the oscillations (overloading). Also, the temperature sensitivity of SAW devices is very high.

SAW microbalances are in an early stage of development and have been used in research applications only. They have been used primarily in stratospheric rockets to sample very dilute aerosols, and have been employed in the measurement of chemical vapor deposition coatings and air pollution chemical reactions (Bowers and Chuan 1989). In the last application, the crystal may be coated with a thin layer of a chemical, solid, or liquid, which then reacts with a selected gas to change the mass of material on the surface, enabling a chemist to follow the progress of the reaction. This method of sensitive, dynamic gravimetric analysis may be useful for the detection and, possibly, the identification of trace pollutants. At least one SAW microbalance (Model 200-1, Femtometrics, Costa Mesa, CA) is now available commercially (Table 14-3).

TAPERED-ELEMENT OSCILLATING MICROBALANCE METHOD

Measurement Principles

TEOM® devices are like piezoelectric crystal devices only in that mass is collected on a vibrating collection substrate, changing its frequency of oscillation. Figure 14-7 shows a typical arrangement for a TEOM® instrument. Instead of a peizoelectric crystal, the active element of any TEOM® system is a specially tapered hollow tube constructed of an elastic, glass-like material. The wide end of the tube is firmly mounted on a relatively massive base plate. The narrow end supports a replaceable collection medium such as a filter or impaction plate and is made to oscillate. Particle-laden gas streams are drawn through the collection medium, where particles are deposited. The filtered gas is then

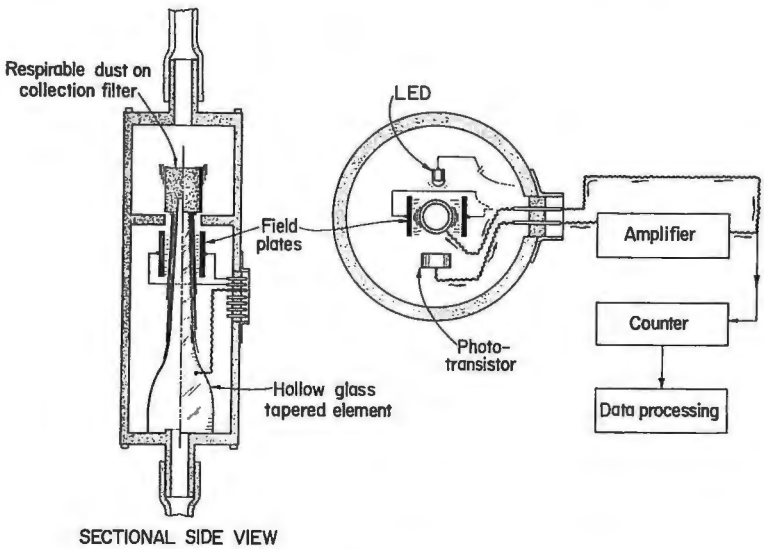

FIGURE 14-7. Typical Arrangement for TEOM® Dust Sensor.

ough the hollow tube, typically
led by an automatic mass flow con-

ctronic feedback system initiates and
ains the oscillation of the tapered ele-
In 1983, the U.S. Bureau of Mines
and the National Institute of Occupa-
Safety and Health (NIOSH) funded the
elopment of a prototype TEOM® dust
for mining applications (Patashnick
Rupprecht 1983). In that particular de-
ght-emitting diode (LED)–photo-
sistor pair aligned perpendicular to the
of oscillation of the tapered element
the frequency of oscillation. The light-
ocking effect of the oscillating element posi-
ed between the phototransistor and the
LED modulates the output signal of the
phototransistor, which is then amplified. Part
of the amplified signal is applied to a conduc-
tive coating on the outside of the tapered
element. In the presence of constant electric
field plates, this signal provides sufficient
force to keep the tapered element in oscil-
lation. In other words, part of the amplified
signal from the LED–phototransistor pair is
used in an electrical feedback loop to over-
come any amplitude damping of the tapered-
element oscillation. The other part of the
amplified signal from the LED–phototran-
sistor pair is sent to a counter and data
processing stage. Here, the oscillation fre-
quency of the tapered element is calculated
and stored in memory. The manufacturer has
made several proprietary improvements to
the feedback system since the early BOM/
NIOSH prototype.

The equation that describes the behavior
of the TEOM® system derives from the
equations of motion for a simple harmonic
oscillator:

$$\Delta m = K_0\left(\frac{1}{f_b^2} - \frac{1}{f_a^2}\right) \qquad (14\text{-}6)$$

where Δm is the mass of the collected sample,
f_b is the frequency of the oscillating element
after sample collection, f_a is the frequency
before sample collection, and K_0 is a constant
(spring constant) unique to each tapered ele-
ment. As the collection medium collects dust, the mass increases, thereby decreasing the frequency of oscillation. By measuring only the change in frequency, one can determine the gain in the mass of dust on the collection medium. Although this expression for Δm is nonlinear, it is monotonic (single-valued), independent of m, and depends only on the constant K_0. For subsequent measurements, f_b becomes f_a, a new initial frequency that reflects the total mass of the system. The new f_b after sampling will differ from f_a only because of the new mass uptake, Δm, collected during sampling.

Instrument Design

A TEOM® instrument can be tailored for a particular application. To do so, the manufacturer must know the minimum mass concentration the instrument must measure, how quickly each measurement must be made, and what sampling air flow rate will be used. To employ the highest sensitivity for a particular application, the manufacturer must consider the total mass of the tapered-element load. This mass, which in most applications is primarily the filter cartridge, must be held to a minimum to effect the maximum frequency change with a sample mass deposit. The reduction of the filter mass has practical limits that are related to both flow rate and filter life. A filter cartridge must have reasonable dimensions to sustain the desired flow before loading to a point where the flow drops to an unacceptable level. In addition to the filter mass, the tapered element has a certain amount of mass that also contributes to the total mass of the oscillating system. The limits on this mass depend on the dimensions of the tapered element. The element must have a sufficiently wide bore to allow the desired flow with minimum pressure drop and also have sufficient wall thickness to support the filter cartridge.

Potential Biases

Because TEOM® devices operate on vibrational principles like piezoelectric crystal

techniques, it is instructive to examine the TEOM® technology in the light of biases that affect QCM measurements.

Calibration

Calibration for TEOM® instruments is equivalent to determining the spring constant K_0. Since K_0 is determined by the physical characteristics of the tapered element, calibration is not likely to change over a period of time. The manufacturer provides a value of K_0, but the user can easily check the value of K_0 by adding a known mass to the tapered element, measuring the change in oscillation frequency and using Eq. 14-6 to determine K_0. Using this method, Shore and Cuthbertson (1985) found that the manufacturer-supplied value for K_0 was correct within the experimental error. However, they also checked the calibration by injecting known masses of dioctyl phthalate (DOP) over the surface of the collection filter. This method suggested that the TEOM® instrument read particulate masses up to 10% lower (on an average) when the K_0 value supplied by the manufacturer was used. However, the masses of DOP used were much higher than those expected during particulate collection. They also observed that limiting injections to the center of the filter influenced the measurements. These results suggest that if one elects to verify the manufacturer-supplied K_0, aerosol depositions similar to those expected during sampling should be used.

Particle Size Effects

Since TEOM® devices typically use a filter collection medium, collection efficiency will not be significantly affected by particle size. Particles not collected by the filter medium would not represent significant mass. Particle size is likely to be more important to inlet bias of the sampling head; however, these problems are common to all sampling devices and not just to TEOM® measurement technology.

Adherence Effects

Tapered elements typically oscillate at several hundred Hz, rather than at several MHz as is typical of piezoelectric crystals. Furthermore, the collection medium is typically a filter rather than a smooth, hard surface. For these reasons, coupling of the collected aerosol is not usually an issue for TEOM® instruments. Theoretically, if sufficient mass were collected on the TEOM® filter, particles begin to flake off. In practice, however, the filters would clog before collecting particle loadings large enough to cause flaking. In fact, most TEOM® instruments provide a warning suggesting when to replace the filter.

Overloading

If the collection filter became sufficiently loaded, the added mass could conceivably damp the oscillations beyond the ability of the feedback system to sustain them. This situation, called saturation, could introduce serious error. The dynamic range of TEOM® instruments, however, is several orders of magnitude. As discussed in previous section, filters would clog before collecting particle loadings large enough cause saturation.

Particle Losses

As discussed under particle size effects, TEOM® instruments are subject to wall losses or particle losses because of inlet bias. A careful design of the sampling train is, as always, important. Visual wall losses were observed during a test of a prototype TEOM® device designed for personal exposure monitoring in mining environments (Williams and Vinson 1986), but these losses were later attributed to charges on the particles introduced by the test dust generation system.

Damping

If the mass of the support structure for the element is sufficiently small, the element may induce vibrations in the structure itself. The oscillation of the tapered element then will be slightly damped. This phenomenon was observed when testing the prototype TEOM® personal sampler for miners (Williams and Vinson 1986). Such damping will not be significant if the mass of the support structure is much larger than the mass of the element, or if

the support structure is properly clamped to a large mass. Tests of the prototype TEOM® personal sampler for miners represent a special case; damping of this sort has not been reported for the commerical TEOM® instruments.

Results and Applications

The TEOM® technology had its beginnings at Dudley Observatory in the 1960s in conjunction with micrometeorite research (Patashnick and Hemenway 1969). A microbalance, at that time consisting of a thin quartz fiber, was designed to measure particle masses in the range 10^{-5}–10^{-11} g. Since that time, its inventors have made many improvements to the quartz fiber approach, and formed Rupprecht & Patashnick (R&P) Co., Inc. to market the device. R&P is currently the only manufacturer and vendor of TEOM® instruments.

R&P provides a variety of instruments that use the TEOM® technology, but only three are within the scope of this book. The first, the Series 1100 monitor, has been used in a variety of applications involving higher-than-ambient conditions. Many leading diesel engine manufacturers throughout the world have used the TEOM® technology in the design and development of engines. Particulate emissions from many vehicles using diesel engines must meet legislated standards in the United States. Regulations require making measurements of particulate emissions while operating the engine over a prescribed wide range of conditions. The near-real-time measurements possible with TEOM® instruments allow designers to identify those engine conditions that contribute most to emissions. In fact, vehicle-to-vehicle differences in transient particulate emissions are readily detected by the TEOM® instrument (Shore and Cuthbertson 1985). The TEOM® instrument has been demonstrated to have a one-to-one response to mass (Whitby, Johnson, and Gibbs 1985); however, care must be taken to properly account for volatile species.

Several research organizations have used the Series 1100 to measure changing concentrations in near-real-time. The BOM, in studying the health and safety hazards of materials burning in underground mine fires, used a TEOM® instrument to help study smoke characteristics. The BOM monitored the mass concentrations of smoke from wood (Egan and Litton 1986) and electrical transformer fluid (Egan 1986) fires. Newman and Steciak (1987) used the TEOM® instrument to help characterize smoke properties for fire modeling, fire detector evaluation, and assessment of the nuclear winter problem.

The Series 1200 monitor is meant primarily for research and indoor industrial applications. The Series 1400 is an industrially hardened version, better suited to remote monitoring situations. The Environmental Protection Agency has certified both instruments for PM-10 measurements of ambient air quality (U.S. Environmental Protection Agency 1989).

References

Bowers, W. D. and R. L. Chuan. 1989. Surface acoustic-wave piezoelectric crystal aerosol mass monitor. *Rev. Sci. Instr.* 60(7):1297–302.

Cooper, D. W. 1975. Statistical errors in beta absorption measurements of particulate mass concentration. *J. Air Poll. Control Assoc.* 25:1154.

Cooper, D. W. 1976. Significant relationships concerning exponential transmission or penetration. *J. Air Pollut. Control Assoc.* 26:366.

Courtney, W. J., R. W. Shaw, and T. C. Dzubay. 1982. Precision and accuracy of beta gauge for aerosol mass determinations. *Environ. Sci. Tech.* 16:236.

Egan, M. R. 1986. Transformer fluid fires in a ventilated tunnel. *BuMines* IC 9117.

Egan, M. R. and C. D. Litton. 1986. Wood crib fires in a ventilated tunnel. *BuMines* RI 9045.

Evans, R. D. 1955. *The Atomic Nucleus.* New York: McGraw-Hill.

Fairchild, C. I., M. I. Tillery, and H. J. Ettinger. 1980. An Evaluation of Fast Response Aerosol Mass Monitors. Los Alamos National Laboratory, Report LA-8220.

Fairchild, C. I. and L. D. Wheat. 1984. Calibration and evaluation of a real-time cascade impactor. *Am. Ind. Hyg. Assoc. J.* 45(4):205–11.

Gleason, G. I., J. D. Taylor, and P. L. Tabern. 1951. Absolute beta counting at defined geometries. *Nucleonics* 8:12.

Heintzenberg, J. and P. Winkler. 1984. Elemental carbon in the urban aerosol. *Sci. Tot. Environ.* 36:27.

Husar, R. B. 1974. Atmospheric particulate mass monitoring with a beta radiation detector. *Atmos. Environ.* 8:183.

Jaklevic, J. M., R. C. Gatti, F. S. Goulding, and B. W. Loo. 1981. A beta gauge method applied to aerosol samples. *Environ. Sci. Tech.* 15:680.

Jaklevic, J. M., N. W. Madden, and C. E. Wiegand. 1983. A precision beta gauge using a plastic scintillator and photomultiplier detector. *Nucl. Inst. and Methods* 214:517.

Karasek, F. W. 1978. Cascade particle analyzer. *Industr. Res./Develop.*:154–58.

Klein, F., C. Ranty, and L. Sowa. 1984. New examinations of the validity of the principle of beta radiation absorption for determinations of ambient air dust concentrations. *J. Aerosol Sci (U.K.)* 15:391.

Lilienfeld, P. 1975. Design and operation of dust measuring instrumentation based on the beta-radiation method. *Staub-Reinhalt Luft* 35:458.

Lippmann, M. 1978. Respirable dust sampling. In *Air Sampling Instruments for Evaluation of Atmospheric Contaminants*, 5th edn., pp. G1–G23, Cincinnati: American Conference of Government Industrial Hygienists.

Loo, B. W., W. R. French, R. C. Gatti, F. S. Goulding, J. M. Jaklevic, J. Llacer, and A. C. Thompson. 1978. Large-scale measurement of airborne particulate sulfur. *Atmos. Environ.* 12:759.

Lundgren, D. A., L. D. Carter, and P. S. Daley. 1976. Aerosol mass measurement using piezoelectric crystal sensors. In *Fine Particles*, ed. B. Y. H. Liu, pp. 485–510. New York: Academic Press.

Macias, E. S. and R. B. Husar. 1970. High resolution online aerosol mass measurement by the beta attenuation technique. In *Proc. 2nd Internat. Conf. on Nucl. Methods in Environ. Research*, ed. J. R. Vogt and W. Meyer, pp. 413. CONF-740701.

Newman, J. S. and J. Steciak. 1987. Characterization of particulates from diffusion flames. *Combustion and Flame* 67(1):55–64.

Patashnick, H. and C. L. Hemenway. 1969. Oscillating fiber microbalance. *Rev. Sci. Instr.* 40(8):1008–11.

Patashnick, H. and G. Rupprecht. 1983. Personal dust exposure monitor based on the tapered element oscillating microbalance. *BuMines* OFR 56–84, NTIS PB 84-173749.

Rose, W. I. Jr., R. L. Chuan, R. D. Cadle, and D. C. Wood. 1980. Small particles in volcanic eruption clouds. *Am. J. Sci.* 280:671–96.

Sem, G. J. and J. W. Borgos. 1975. An experimental investigation of the exponential attenuation of beta radiation for dust measurements. *Staub-Reinhalt Luft* 35:5.

Sem, G. J. and K. Tsurubayashi. 1975. A new mass sensor for respirable dust measurement. *Am. Ind. Hyg. Assoc. J.* 36(11):791–99.

Shore, P. R. and R. D. Cuthbertson. 1985. Application of a tapered element oscillating microbalance to continuous diesel particulate measurement. *Soc. Automotive Eng.*, Report 850, 405.

Spengler, J. D. and G. D. Thurston. 1983. Mass and elemental composition of fine and coarse particles in six U. S. cities. *J. Air Pollut. Control Assoc.* 33:1162.

Stevens, R. K., T. G. Dzubay, R. W. Shaw Jr., W. A. McClenny, C. W. Lewis, and W. E. Wilson. 1980. Characterization of the aerosol in the Great Smoky Mountains. *Environ. Sci. Technol.* 14:1491.

U.S. Environmental Protection Agency. 1989. Compendium Method IP-10B: Determination of Respirable Particulate Matter in Indoor Air Using a Continuous Particulate Monitor.

Wallace, D. and R. Chuan. 1977. A Cascade Impactor Instrument Using Quartz Crystal Microbalance Sensing Elements for Real-Time Particle Size Distribution Studies. *National Bureau of Standards Special Publication 464.*

Ward, M. D. and D. A. Buttry. 1990. *In situ* interfacial mass detection with piezoelectric transducers. *Science* 249:1000–07

Whitby, R., R. Johnson, and R. Gibbs. 1985. Second Generation TEOM Filters—Diesel Particulate Mass Comparisons between TEOM and Conventional Filtration Techniques. *Soc. Automotive Eng.*, Paper 850, 403.

Williams, K. L. and R. P. Vinson. 1986. Evaluation of the TEOM dust monitor. BuMines IC 9119.

AEROSOL MEASUREMENT

Principles, Techniques, and Applications

Edited by
Klaus Willeke
Paul A. Baron

VNR VAN NOSTRAND REINHOLD
New York